First principles multiplet calculations of the calcium $L_{2,3}$ x-ray absorption spectra of CaO and CaF_2

2011 J. Phys.: Condens. Matter 23 145501

(http://iopscience.iop.org/0953-8984/23/14/145501)

J. Phys.: Condens. Matter **23** (2011) 145501 (7pp) doi:10.1088/0953-8984/23/14/145501

First principles multiplet calculations of the calcium $L_{2,3}$ x-ray absorption spectra of CaO and CaF_2

P S Miedema[1], H Ikeno[1,2] and F M F de Groot[1]

[1] Department of Inorganic Chemistry and Catalysis, Debye Institute for Nanomaterials Science, Utrecht University, Sorbonnelaan 16, 3584 CA Utrecht, The Netherlands
[2] Fukui Institute for Fundamental Chemistry, Kyoto University, Takano-Nishihiraki-cho 34-4, Sakyo-ku, Kyoto 606-8103, Japan

Received 30 January 2011, in final form 22 February 2011
Published 22 March 2011
Online at stacks.iop.org/JPhysCM/23/145501

Abstract
First principles calculations are performed for the interpretation of the $L_{2,3}$ x-ray absorption spectrum of calcium oxide and calcium fluoride. The first principles calculations are based on configuration interaction (CI) calculations using fully relativistic molecular spinors. The first principles results are compared to experimental data and also to calculations based on a semi-empirical crystal field multiplet model and also on a multichannel multiple scattering method. We show that the CI calculations show good agreement with experiment, both for bulk and for surface experiments. The remaining differences with experiment and between the theoretical models are discussed in detail.

(Some figures in this article are in colour only in the electronic version)

1. Introduction

The calculation of core level spectra has a long history [1]. The x-ray absorption (XAS) spectral shape is described as the transition from a core state to an empty state. If one excites an electron from a 1s core state one can describe the XAS spectral shape essentially as probing the empty density of states in the presence of a core–hole. A large range of first principle calculations are based on this approach, including multiple scattering, band structure calculations and quantum chemical calculations. In addition to the well-known problems of the respective ground state calculations, the calculation of core excited states is further complicated by the usage of models and approximations to describe the core excitation.

The metal $L_{2,3}$ edge XAS of transition metal elements are strongly affected by multiplet effects, the overlap of the 2p and 3d wavefunctions yielding large two-electron integrals for the coupling between the core 2p and valence 3d states. Due to the large multiplet effects, the $L_{2,3}$ XAS spectra deviate significantly from the ground state density of states. It turns out to be not enough to describe the core–hole as an extra potential, but it is necessary to treat its full wavefunction character in the interpretation of the $L_{2,3}$ XAS spectral shape. Over the last 25 years, the transition metal $L_{2,3}$ edges have been successfully simulated with crystal field multiplet (CFM) and charge transfer multiplet (CTM) models [1]. The CFM and CTM models can accurately describe most $L_{2,3}$ XAS spectra, but they need one or more empirical parameters in such simulations. In this work we will focus on the possibilities to calculate metal $L_{2,3}$ edges of transition metal systems from first principles calculations. We have chosen CaO and CaF_2 as test cases, because calcium (Ca) $L_{2,3}$ calculations have been published using both CFM calculations [2] and multichannel multiple scattering (MCMS) calculations [3]. Recently, a number of first principles calculations have been published for systems with a band gap between the filled oxygen 2p-band and the empty 3d-band, in particular for TiO_2. Both MCMS [4] and Bethe–Salpeter [5] have reached good agreement for the titanium $L_{2,3}$ edge of TiO_2 systems. Both MCMS and Bethe–Salpeter are, as yet, limited to systems with an empty 3d-band in the ground state, as in this case TiO_2 containing $3d^0$ Ti^{4+} ions.

The CaF_2 and CaO spectra have a simple cubic unit cell with a band gap between the ligand 2p and the calcium 3d-band. This yields a relatively straightforward ground state calculation. The empty 3d-band implies that the final state contains a $2p^53d^1$ configuration which has clearly separated peaks, allowing a detailed analysis. From such analysis, we

intend to pinpoint some remaining differences between the first principles simulations and the experimental spectra, with the goal to further improve the accuracy of the first principles simulations. We will compare the calculations performed with the first principles configuration interaction (CI) method [6–8] with the semi-empirical calculations. In addition, we will compare them with the results from the published MCMS method [3].

For the two above mentioned compounds, we will focus on the 2p XAS spectra of three calcium systems.

(1) CaO, octahedral Ca in a rock salt structure.
(2) CaF_2, an ionic Ca system with Ca in an eight-fold cubic symmetry.
(3) The (111) surface of CaF_2 in order to study surface effects.

Calcium oxide, lime, is a crystalline mineral that exists in the rock salt structure, implying that a calcium atom is surrounded by six oxygen ligands. CaF_2 has the so-called fluorite structure. The Ca^{2+} ions in this structure are surrounded by eight fluorine atoms in a cubic symmetry. The calcium atoms at the $CaF_2(111)$ surface can be assumed to have one of its eight surrounding fluorine ions missing, in other words the surface is fluorine terminated. Surface relaxation effects do not give large differences from bulk values for Ca–F distances [9–14], so no changes in the unit cell parameters from the bulk CaF_2 to the surface CaF_2 have to be taken into account in simulation of surface $CaF_2(111)$. Shi *et al* found that the $CaF_2(111)$ surface is the most stable with reference to $CaF_2(110)$ and (100) surfaces [10]. Experimental 2p XAS of CaF_2 and CaF_2/Si(111) showed that the energy positions and relative intensities of both samples agree, except for one extra peak at the L_2-edge. This peak was originally attributed to photon damage, possibly through photo-desorption of F atoms near the sample surface [15]. Himpsel *et al* made clear that the peak near the L_2-edge was a so-called surface effect by using bulk Auger and ion detection modes [2]. Rieger *et al* suggested that at the CaF_2/Si(111) interface, the oxidation state of the Ca atoms is modified to 1+ [16].

2. Theory section

In this section we describe the methods that we have used for the XAS calculations: the semi-empirical CFM method in section 2.1 and the first principles CI method in section 2.2. Our results are compared with the MCMS method, which will be described in section 2.3.

2.1. The semi-empirical crystal field multiplet (CFM) method

The ground state of the calcium in CaO and CaF_2 is Ca^{2+} ($2p^6 3d^0$) $^1S_0$, where the non-acting electrons in the $L_{2,3}$-excitation process (1s, 2s, 3s, 3p) are neglected. In the final state of the x-ray absorption process, an electron is excited from the 2p-core level to the 3d and the 4s states in the dipole approximation. Since the transition to the 3d states is a hundred times stronger than to the 4s states, the transitions to 4s states are neglected in the calculations. According to the selection rules ($\Delta J = 0, \pm 1$ and $J = J' \neq 0$), the states that can be reached in atomic symmetry are $^1P_1$, $^3D_1$ and $^3P_1$. A eight-fold cubic and also an octahedral surrounding (both of O_h symmetry) modifies the transition matrix element from (atomic) $\langle ^1S_0|\text{dipole}|^1P_1\rangle$ to (cubic) $\langle A_1|T_1|T_1\rangle$. This yields seven final states of T_1 symmetry, in other words there are seven peaks in a transition for a calcium ion in cubic symmetry.

XAS calculations as performed in [2] were performed using the CFM model. This approach includes both electron–electron interactions and spin–orbit coupling for each open sub-shell of one atom. For simulation of the spectra, atomic Slater–Condon parameters are used, which are assumed to be 80% of their Hartree–Fock calculated values [17]. The Ca $L_{2,3}$ spectra are calculated from the sum of all possible transitions for an electron excited from the 2p-core level into an unoccupied 3d level. In the crystal field limit the ground state is approximated by a single electronic configuration $3d^0$. The $2p^5 3d^1$ final state is affected by the 2p3d multiplet coupling, the 2p and 3d spin–orbit couplings and the crystal field potential in O_h symmetry. The strength of the crystal field is described as an empirical parameter 10 Dq and that is optimized to experiment [18]. Recently a new interface program was written for the usage of charge transfer multiplet calculations [19].

2.2. First principles configuration interaction (CI) method

The first principles CI method is applied to the calculation of 3d transition metal (TM) $L_{2,3}$ XAS. This method is equivalent to quantum chemical configuration interaction method using fully relativistic molecular spinors. A relativistic density functional theory (DFT) calculation is made using model clusters. Electronic correlations among 3d electrons and a 2p hole were rigorously calculated by taking the Slater determinants made by the DFT-MOs mainly composed of TM 2p and TM 3d spinors. The electronic correlations among TM 3d electrons and 2p core–hole are explicitly calculated [6]. The agreement between experimental and theoretical spectra is better when ligand p orbitals are included in the configuration interaction scheme [6–8]. The relativistic CI method used in the present work is the all-electron CI method. That means, not only the TM 2p, 3d and ligand p spinors, but also other core spinors are considered explicitly to construct Slater determinants.

The CI method is used to calculate the Ca $L_{2,3}$ XAS for calcium oxide (CaO) and calcium difluoride (CaF_2). The bulk crystals are simulated using the structure data from the website [20], card numbers 1549 and 2591. CaF_2 has a lattice constant of 5.4630 Å and CaO has a lattice constant of 4.8105 Å. For XAS calculations on the (111)-plane of CaF_2, the structure data of fluorite were reshaped to a hexagonal cell and the (111) surface was assumed to be fluorine terminated. For the XAS calculations of CaO a cluster of CaO_6^{10-} is used. CaF_2 is calculated with a CaF_8^{6-} cluster and the $CaF_2(111)$ surface with a CaF_7^{5-} cluster. Only the molecular spinors mainly composed of Ca 2p ($\varphi_{\text{Ca 2p}}$) and Ca 3d ($\varphi_{\text{Ca 3d}}$) atomic spinors were considered as active space. The other spinors, $\varphi_{\text{Ca 1s}}$, $\varphi_{\text{Ca 2s}}$, $\varphi_{\text{Ca 3s}}$, $\varphi_{\text{Ca 3p}}$, $\varphi_{\text{O(F) 1s}}$, $\varphi_{\text{O(F) 2s}}$, $\varphi_{\text{O(F) 2s}}$ are treated as a frozen core which were always fully occupied

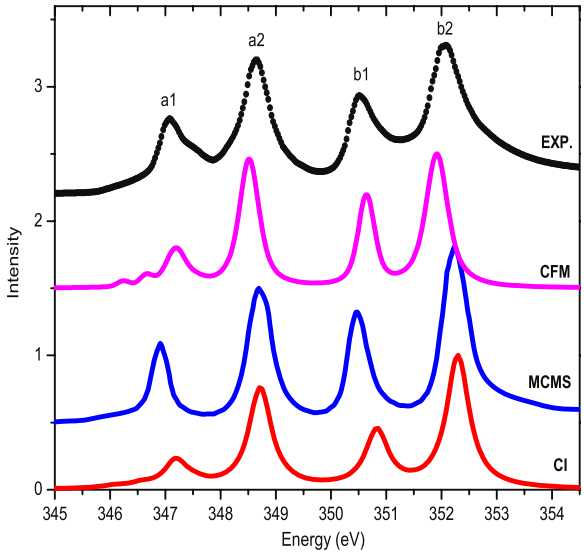

Figure 1. Ca 2p XAS of CaO with, from top to bottom, the experimental spectrum (black), the CFM calculation [2] (pink), the MCMS calculation [3] (blue) and the CI calculation (red). The most important peaks are indicated with the symbols a_1, a_2, b_1 and b_2.

by electrons. Since the Ca $L_{2,3}$ XAS is mainly ascribed to the transition between $(\varphi_{\text{Ca 2p}})^6(\varphi_{\text{Ca 3d}})^0$ and $(\varphi_{\text{Ca 2p}})^5(\varphi_{\text{Ca 3d}})^1$ configurations, Slater determinants corresponding to these two configurations were considered to describe the initial and the final state wavefunctions. Thus the number of Slater determinants for the initial and the final states for XAS were 1 and 60, respectively. The exchange–correlation interactions among $\varphi_{\text{Ca 2p}}$ and $\varphi_{\text{Ca 3d}}$ electrons were rigorously calculated. In addition, the inter-electron interaction among $\varphi_{\text{Ca 2p}}/\varphi_{\text{Ca 3d}}$ electrons and other core electrons was explicitly taken into account. Since this calculation produces sticks, an adjustable parameter for the broadening of the spectrum is needed. In this study we use a Lorentzian broadening of 0.3 eV for the whole spectrum of CaF_2 and 0.5 eV for the whole spectrum of CaO.

2.3. Multichannel multiple scattering (MCMS) method

Krüger *et al* have calculated the XAS of CaO and CaF_2 using a MCMS approach [3]. The MCMS theory was developed by Natoli *et al* [22] as a multiple scattering approach to correlated N-electron wavefunctions. The studied system is divided in the absorber atom with the strongly correlated N-electron wavefunctions and the other (surrounding) atoms as environment. The correlated N-electron wavefunction, with a finite number N, contains at most one electron in a delocalized orbital and the rest of the electrons are in localized orbitals. All other electrons of the atoms in the environment are described within the independent particle approximation, where the reflectivity of the environment can be calculated using a single-channel multiple scattering. What remains is the calculation of the multichannel matrix of the absorber with the N electrons, with a (partial) screening of the core–hole potential. As yet, the MCMS theory has only been applied to systems without electrons in the 3d-band in the ground state [3, 4, 21].

Table 1. From left to right are given the method, the energy difference $b_2 - b_1$, the intensity ratio at the L_2 edge $(b_1/(b_1 + b_2))$. The fourth column gives the energy difference $b_2 - a_2$ in eV and the fifth column is the $L_3/(L_2 + L_3)$ area ratio. The experiment is compared with the CI and MCMS methods and the CFM calculation with a 10 Dq of 1.2 eV and the Slater integrals at 80% of the Hartree–Fock values. The last row is an optimized CFM calculation with a 10 Dq of 1.4 eV and the Slater integrals set to 90% of the Hartree–Fock values.

Method	b_2-b_1 (eV)	$b_1/(b_1+b_2)$ [0, 1]	b_2-a_2 (eV)	$L_3/(L_2+L_3)$ [0, 1]
Exp	1.53	0.24	3.40	0.38
CI	1.51	0.31	3.60	0.42
MCMS	1.76	0.30	3.57	0.37
CFM (1.2)	1.34	0.28	3.42	0.38
CFM (1.4)	1.53	0.30	3.43	0.38

In this paper we compare the spectra as calculated with the CI method with spectra obtained from experiment as well as with semi-empirical CFM calculations and the published MCMS theoretical spectra.

3. Results

The results section is divided in the simulations of the 2p XAS of CaO (section 3.1), the 2p XAS of bulk CaF_2 (section 3.2) and the 2p XAS of surface CaF_2 (section 3.3).

3.1. 2p XAS of CaO

In figure 1 the CI-calculated XAS of CaO is shown in comparison with the experimental $L_{2,3}$-edge of calcium oxide powder, the MCMS calculation and a CFM multiplet calculation with 10 Dq = 1.2 eV. We have labeled the four main peaks with a_1, a_2, b_1 and b_2. The L_3 edge contains the a_1 and a_2 peaks, which can be correlated with mainly t_{2g} and e_g respectively. The b_1 and b_2 peaks are their L_2 analogs. Both first principles calculations as well as the CFM calculation simulate the experiment well. To make the comparison more quantitative, we will make a comparison between energy differences and intensity ratio between the peaks. We have chosen four characteristic numbers to quantify the calculations. The energy difference between b_2 and b_1 $(b_2 - b_1)$ and also the intensity ratio between these two peaks are both related to the crystal field splitting. The Slater integrals allow the mixing of $2p \rightarrow t_{2g}$ and $2p \rightarrow e_g$ transition channels. Without Slater integrals the $b_1/(b_1 + b_2)$ ratio is 0.6. The larger the Slater integrals are the smaller this ratio will be. The other parameters are the intensity ratio between L_3 and L_2 with $L_3/(L_2 + L_3)$ and the energy difference between b_2 and a_2 $(b_2 - a_2)$, which is a measure for the distance between the L_3 and L_2 peaks and therefore for the 2p spin–orbit coupling.

Table 1 shows the four characteristic numbers of the $L_{2,3}$ edge compared with the theoretical numbers. Compared with experiment, the CI calculations find a similar $b_2 - b_1$ distance, which indicates that the crystal field strength is calculated correctly. For the CI method, the crystal field splitting at Ca 3d levels can be obtained as the difference between averaged

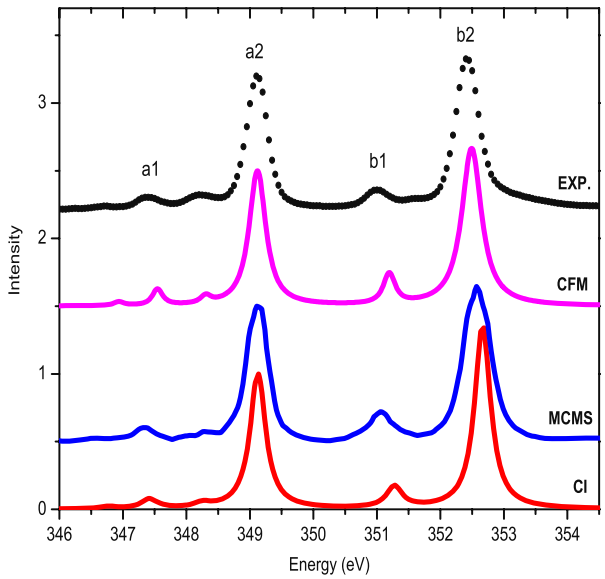

Figure 2. Ca 2p XAS of CaF_2 with, from top to bottom, the experimental spectrum (black), the CFM calculation [2] (pink), the MCMS calculation [3] (blue) and the CI calculation (red). The most important peaks are indicated with the symbols a_1, a_2, b_1 and b_2.

eigenvalues of t_{2g} and e_g molecular spinors. This is 1.45 eV for the CaO_6^{10-} cluster of CaO which is almost the same as the optimized 10 Dq value in CFM model as described below. The MCMS calculation finds a too large $b_2 - b_1$ distance indicating a too large crystal field effect. The ratio of the two L_2 peaks is a bit larger in the first principles calculations than in experiment. The branching ratio is correct in MCMS and a bit too large in CI. A remarkable result is that the $b_2 - a_2$ distance is too large in the MCMS and CI calculations, even though the 2p-core spin–orbit coupling is explicitly taken into account by solving the Dirac equation. The overestimation of $b_2 - a_2$ distance in our CI simulations could be ascribed to the fact that the relativistic effects on electron–electron interactions were not taken into account in the present calculations. The effect of Breit interaction, which is the first relativistic correction to the electron–electron interactions, have been discussed elsewhere [22]. If the Breit interaction is taken into account, the $b_2 - a_2$ distance might approach the value of the $b_2 - a_2$ distance of the experimental result.

The CFM calculations allow the manipulation of all the different factors that generate the spectral shape. We start with the assumption that all atomic parameters are as calculated for a Ca^{2+} ion, using the 80% reduction of the Hartree–Fock values [17]. Increasing the crystal field value 10 Dq increases the $b_2 - b_1$ distance and also the $b_1/(b_1 + b_2)$ peak ratio. The experimental $b_2 - b_1$ distance is found for a 10 Dq value of 1.4 eV, but this yields a $b_1/(b_1 + b_2)$ peak ratio that is too high. We corrected the $b_1/(b_1 + b_2)$ peak ratio by increasing the Slater integrals to 90% of their Hartree–Fock values for 10 Dq = 1.4 eV. This yields the correct $b_2 - b_1$ distance and almost the correct $b_1/(b_1 + b_2)$ peak ratio. Also the branching ratio is exactly correct for this parameter set. This simulation suggests that the Slater integrals for CaO should not be reduced to 80% of their Hartree–Fock value but only to 90%. Note that the CaO calculation only involves the 2p3d Slater integrals.

Table 2. 2p and 3d spin–orbit coupling and Slater 2p3d integrals of the CFM method and the CI method.

	CFM[a]	CI[b]
2p spin–orbit coupling (eV)	2.40	2.46
3d spin–orbit coupling (eV)	0.011	0.014
F^2 Slater integrals (eV)	3.04	3.48–3.54[c]
G^1 Slater integrals (eV)	2.01	2.27–2.32[c]
G^3 Slater integrals (eV)	1.14	1.29–1.32[c]

[a] For CFM, the Slater integrals shown are the reduced Hartree–Fock values, to 80% of their original values.

[b] For CI, the energies of the 2p orbitals were averaged: $2p_{avg} = (2p_{1/2} + 2 \times (2p_{3/2}))/3$; then the $|2p_{avg} - 2p_{1/2}|$ gives an estimate for the 2p spin–orbit coupling. It should be noted that this estimate is an 'effective' spin–orbit coupling. This value also includes some relativistic effects other than spin–orbit coupling. The 'effective 3d spin–orbit coupling' is estimated from the energy splitting of t_{2g} levels.

[c] The Slater integrals for CI are set as a range because the values of the Slater integrals slightly differ for different 2p3d combinations.

The CFM and CI values for the 2p spin–orbit coupling, 3d spin–orbit coupling and the Slater integrals are shown in table 2. The values for the (effective) 2p and 3d spin–orbit coupling are almost the same for CFM and the CI calculation. However the Slater integral values are different in the CFM and CI calculation. The Slater integrals in the CI calculation are always larger than the Slater integrals in the CFM calculation. The values of the CI calculation are roughly compared to 90% of the Hartree–Fock values. The 80% which is commonly used in the CFM calculation is an arbitrary value where also 90% could have been chosen. This has been confirmed by studying the CFM calculation of CaO with 90% of the Slater integrals as mentioned above.

The Slater integrals in the CI calculation are taken from a DFT calculation, where the electronic correlation effects are partially taken into account. However, charge transfer effects which are used in a multiplet calculation for considering the covalent bonding between the metal (Ca) and the ligand (O or F) were not taken into account. In CFM, these covalency effects could also be taken into account by further reducing the Slater integrals. In that sense it could be more reasonable to take the 80% values for the CFM calculation. However, in the present cases of the relative ionic compounds CaO and CaF_2 it seems that 90% Slater integrals give the best simulation result.

3.2. 2p XAS of CaF_2

In figure 2 the experimental XAS of bulk CaF_2 powder and the calculations of Krüger [3], Himpsel *et al* [2] and this study are shown. The main peaks are indicated with the symbols a_1, a_2, b_1 and b_2. At first sight, the agreement between experiment and calculation is rather good for the semi-empirical crystal field multiplet calculation and the calculation by Krüger. The CI calculation is a little off in the L_3 to L_2 distance

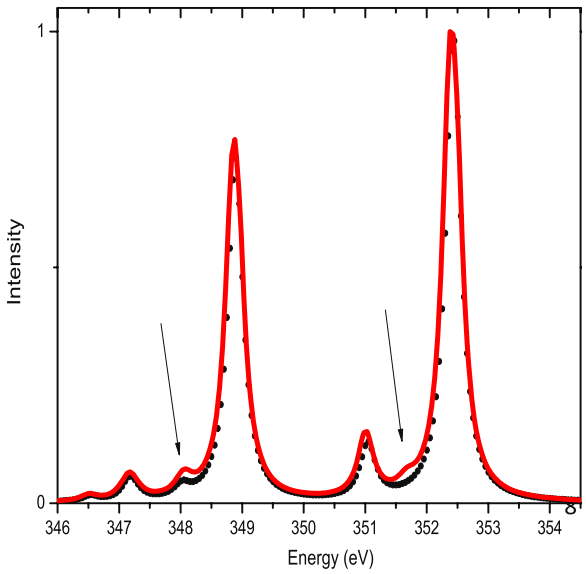

Figure 3. Calculated Ca $L_{2,3}$ edge XAS of bulk CaF_2 (in black, dotted) and of bulk CaF_2 at the 111-orientation in (red, solid) using the CI method.

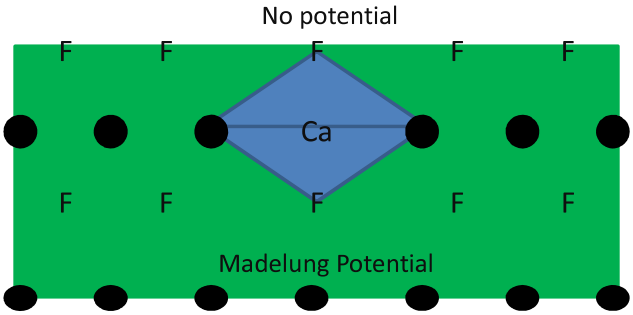

Figure 4. Schematic representation of the CaF_8^{6-} cluster indicated in blue in the 111-orientation with the Madelung potential.

Table 3. From left to right are given the method, the energy difference between b_2 and b_1, the intensity ratio at the L_2 edge ($b_1/(b_1 + b_2)$). The fourth column gives the energy difference $b_2 - a_2$ in eV and the fifth column is the $L_3/(L_3 + L_2)$ ratio for calculations on CaF_2. The CFM calculation with a negative 10 Dq value of −0.75 eV is compared with experiment (Exp) and the CI and MCMS method.

Method	b_2-b_1 (eV)	b_1/b_1+b_2 [0, 1]	b_2-a_2 (eV)	$L_3/(L_2+L_3)$ [0, 1]
Exp	1.44	0.12	3.31	0.43
CI	1.40	0.13	3.55	0.43
MCMS	1.53	0.15	3.45	0.41
CFM	1.33	0.11	3.38	0.42

($b_2 - a_2$). Quantitatively compared in table 3 it is indeed found that for the CI calculation the main difference between the CI calculation and the experiment comes from the difference between the b_2 and a_2 distance of the experimental and the CI-calculated spectrum. For the rest of the quantified parameters, the CI calculation is comparable or better than the MCMS and CFM calculations if compared with the experimental data. In the CI calculation the $b_2 - a_2$ distance is higher, 3.55, than for the experiment, 3.31. As mentioned above for the CI calculation of the XAS of CaO, this difference in $b_2 - a_2$ distance has been ascribed to a Breit interaction [23]. For CaO the difference in this $b_2 - a_2$ distance between experiment and the CI calculation was 0.2 and now for CaF_2 it is 0.24 eV.

3.3. Surface effects in XAS-CaF_2(111) studied with CI multiplet calculations

The surface of CaF_2(111) has been studied by Himpsel *et al* [2], who have shown that near the intense peak of the L_2-edge, a peak concerning surface effects is visible. Smaller effects are found in the low-energy shoulder of the main L_3-peak. To simulate the CaF_2(111), we have used the hexagonal lattice of CaF_2 in which the a*b*-plane is parallel to (111) surface.

In figure 3 the CI calculation for bulk CaF_2 is compared with the calculation for bulk CaF_2 in the (111) orientation. Here, the fluorine deficiency has not been taken into account yet. A small increase of the shoulder peaks of the main L_2 and L_3 edge in the 111-orientation is found and these are indicated with arrows. These increased intensities were ascribed by Himpsel *et al* [2] as surface effects. In our calculation of the CaF_2 in the 111-orientation, we notice that there is symmetry-breaking already. The reason of this symmetry-breaking becomes clear looking at figure 4. The cluster in the 111-orientation is shown with the Madelung potential of the CaF_8^{6-} cluster. The Madelung potential is only on one side of the cluster, for example the negative z axis. That is essentially the symmetry-breaking for the CaF_8^{6-} cluster, on one side a Madelung potential and no potential on the other side. The symmetry-breaking in the (111)-orientation already increases these 'surface peaks' indicated with the arrows. This indicates that a combination of surface effects and symmetry-breaking causes the shoulder peaks in the XAS to increase.

It is assumed that the (111)-surface of CaF_2 is cut between the calcium and fluorine layer. So, we used a CaF_7^{5-} cluster to calculate the XAS of surface CaF_2. In the CI calculation one could calculate the s- and p-polarization of XAS and make a comparison with the experimental observations of Himpsel *et al* [2]. The calculated s- and p-polarized XAS are shown in figure 5.

In the CI calculations all peaks in the s- and p-polarization of the experimental data are reproduced. The energy difference between L_2 and L_3 is, as expected from the discussion above, too large in the calculation.

The semi-empirical crystal field multiplet model could also fit the experimental s- and p-polarized XAS as is shown in [2]. Since the symmetry is lower for a surface, this means the crystal field has to be described by more than one parameter. This could in principle make it possible that more couples of crystal field parameters might be well fitted to the experimental data. In that case, the CI multiplet calculations would have the preference; also in the future for example in calculations on nano-sized systems or for interfaces.

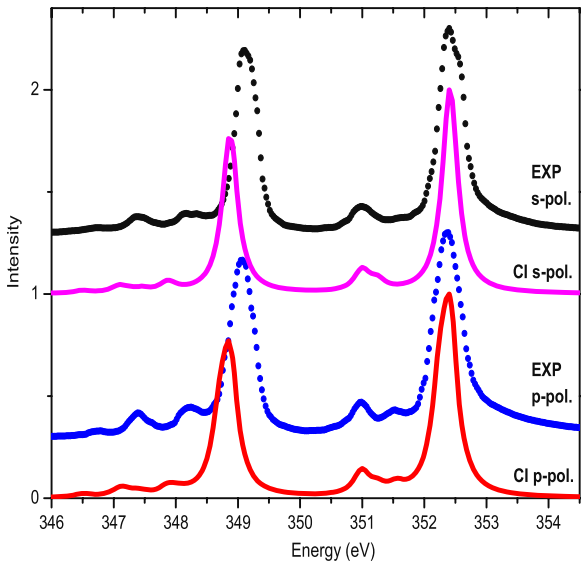

Figure 5. Ca 2p XAS of CaF_2/Si(111) with, from top to bottom, the s-polarized experimental spectrum (black), the s-polarized CI calculation (pink), the p-polarized experimental spectrum (blue) and the p-polarized CI calculation (red).

4. Discussion

The XAS calculations of the Ca $L_{2,3}$-edge for bulk CaO and CaF_2 using the CI method show that there is a discrepancy in the $L_2 - L_3$ distance (indicated above with $b_2 - a_2$) compared to the experimental XAS. Above we have mentioned that one major reason is the neglect of the Breit interaction. In principle, one could include this Breit interaction in the XAS calculation, but at the expense of the costs of the calculation.

We also would like to point out the differences between the semi-empirical CFM and the CI method. The CFM starts from an atomic description described using a Hartree–Fock calculation. The Coulomb and exchange interactions of the interacting electrons in the XAS process (2p and 3d) are considered. Due to the lack of electronic correlation effects, Hartree–Fock overestimates the Slater integrals, which are therefore reduced to 90% or 80% to account for the atomic Slater integrals. The values of the Slater integrals have an important effect on the checked parameters $b_1/b_1 + b_2$, $b_2 - b_1$ and $b_2 - a_2$ distance and the branching ratio $L_3/(L_2 + L_3)$. Then the atom is put into a surrounding by introducing an empirical crystal field energy value.

On the other side, the CI method starts with DFT-calculated spinors of a real-space cluster of atoms. The DFT-calculated spinors already include some correlation and therefore the Ca 2p3d Slater integrals are reduced themselves rather than by an arbitrary number in the CFM calculation. However, the Slater integrals are further reduced if charge transfer effects, which account for covalent bonding between the Ca metal and the oxygen ligands, are included. Again to point out, the main difference with CFM is that with the CI method the XAS is fully calculated from first principles without introducing empirical parameters. This is mainly interesting for calculations on lower-symmetry materials.

Next to the neglect of the Breit interaction, other discrepancies between the experimental spectra and the CI calculation are most likely due to the approximations made in the calculation. These approximations include the size of the cluster with point charges around it, the use of a static cluster and taking into account too high symmetry in the calculation. There might also be non-local effects in an experimental XAS spectrum, which are neither accounted for in the CI model nor in the CFM model. However, even with all the approximations mentioned above one can still predict the XAS multiplet peaks originating from surface effects.

5. Conclusions

The XAS calculations and quantitative analysis of some peak features for calcium oxide (CaO) and calcium fluoride (CaF_2) show that the CI method is comparable or better than the semi-empirical crystal field method and the MCMS method in predicting the experimental spectrum. The effects of surface structures on the Ca-$L_{2,3}$ XAS of CaF_2 could be simulated by the CI method. For compounds that have a local symmetry lower than octahedral or tetrahedral, so for systems with symmetry-breaking, multiplet calculations for L-edge XAS using a first principles or *ab initio* method would have the preference over the CFM model. This is because the CFM model in the lower-symmetry cases needs more empirical parameters.

The suggested surface with a deficiency of fluorine atoms [24, 25] is used in our CI XAS calculations and gives good agreement with the experimental XAS. For studying surface effects in XAS, the calculations with the CI method have advantages over XAS calculations with the semi-empirical crystal field multiplet model, because it is directly calculated from the real-space input which you can obtain from experiments. The main discrepancy between the experimental XAS and the CI-calculated XAS is the $L_2 - L_3$ energy difference. This is ascribed to the neglect of the Breit interaction.

Summarized, the first principles CI method is a powerful real-space method for calculating $L_{2,3}$-edge multiplet XAS of compounds with symmetry-breaking and this method reproduces the multiplet peaks very well.

Acknowledgment

PSM, HI and FMFdeG acknowledge financial support from the Netherlands National Science Foundation (NWO/VICI program).

References

[1] de Groot F M F 2005 Multiplet effects in x-ray absorption *Coord. Chem. Rev.* **249** 31–63
[2] Himpsel F J *et al* 1991 Fine structure of the Ca 2p x-ray-absorption edge for bulk compounds, surfaces, and interfaces *Phys. Rev.* B **43** 6899–907
[3] Krüger P and Natoli C R 2004 X-ray absorption spectra at the Ca $L_{2,3}$ edge calculated within multichannel multiple scattering theory *Phys. Rev.* B **70** 245120

[4] Krüger P 2010 Multichannel multiple scattering calculation of $L_{2,3}$-edge spectra of TiO_2 and $SrTiO_3$: importance of multiplet coupling and band structure *Phys. Rev.* B **81** 125121
[5] Laskowski R and Blaha P 2010 Understanding the $L_{2,3}$ x-ray absorption spectra of early 3d transition elements *Phys. Rev.* B **82** 205104
[6] Ikeno H *et al* 2006 First-principles multi-electron calculations for $L_{2,3}$ ELNES/XANES of 3d transition metal monoxides *Ultramicroscopy* **106** 970–5
[7] Ikeno H *et al* 2005 First-principles multielectron calculations of Ni $L_{2,3}$ NEXAFS and ELNES for $LiNiO_2$ and related compounds *Phys. Rev.* B **72** 075123
[8] Ogasawara K *et al* 2001 Relativistic cluster calculation of ligand-field multiplet effects on cation $L_{2,3}$ x-ray-absorption edges of $SrTiO_3$, NiO, and CaF_2 *Phys. Rev.* B **64** 115413
[9] Vogt J, Henning J and Weiss H 2005 The structure of $CaF_2(111)$ and $BaF_2(111)$ single crystal surfaces: a tensor low energy electron diffraction study *Surf. Sci.* **578** 57–70
[10] Shi H, Eglitis R I and Borstel G 2005 First-principles calculations of the CaF_2 bulk and surface electronic structure *Phys. Status Solidi* b **242** 2041–50
[11] Gotte A *et al* 2007 Theoretical and experimental studies of the structure and dynamics of the $CaF_2(111)$ surface *Surf. Sci.* **601** 411–8
[12] Puchin V E *et al* 2001 Theoretical modelling of steps on the $CaF_2(111)$ surface *J. Phys.: Condens. Matter* **13** 2081–94
[13] Puchina A V *et al* 1998 Theoretical modelling of steps and surface oxidation on $CaF_2(111)$ *Surf. Sci.* **402–404** 687–91
[14] Dabringhaus H 2000 Theoretical study of the adsorption of lithium fluoride molecules at the (111) surface of CaF_2 *Surf. Sci.* **462** 123–34
[15] Chen C T and Sette F 1988 Comment on "Determination of interface states for CaF_2/Si(111) from near-edge x-ray absorption measurements" *Phys. Rev. Lett.* **60** 160
[16] Rieger D *et al* 1986 Electronic structure of the CaF_2/Si(111) interface *Phys. Rev.* B **34** 7295–306
[17] Cowan R D 1981 *The Theory of Atomic Structure and Spectra* (Berkeley CA: University of California Press)
[18] de Groot F and Kotani A 2008 Core level spectroscopy of solids *Advances in Condensed Matter Science* vol 6, ed D D Sarma, G Kotliar and Y Tokura (Boca Raton, FL: CRC Press)
[19] Stavitski E and de Groot F M F 2010 The CTM4XAS program for EELS and XAS spectral shape analysis of transition metal L edges *Micron* **41** 687–94
[20] WWW-MINCRYST 2011 Crystallographic and crystallochemical database for minerals and their structural analogue http://database.iem.ac.ru/mincryst
[21] Natoli C R *et al* 1990 Multichannel multiple-scattering theory with general potentials *Phys. Rev.* B **42** 1944–68
[22] Ikeno H and Tanaka I 2008 Effects of Breit interaction on the $L_{2,3}$ x-ray absorption near-edge structures of 3d transition metals *Phys. Rev.* B **77** 075127
[23] de Groot F M F *et al* 1990 $L_{2,3}$ x-ray-absorption edges of d^0 compounds: K^+, Ca^{2+}, Sc^{3+}, and Ti^{4+} in O_h (octahedral) symmetry *Phys. Rev.* B **41** 928–37
[24] Miura K, Sugiura K and Sugiura H 1991 F^+-desorption mechanism from a $CaF_2(111)$ surface by low-energy electron irradiation *Surf. Sci.* **253** L407–10
[25] Saiki K *et al* 1987 *In situ* observation of defect formation in $CaF_2(111)$ surfaces induced by low energy electron bombardment *Surf. Sci.* **192** 1–10